


Dynamics, statistics, and task allocation of foraging antsNuoya Zhang and Ee Hou Yong ^{*}*Division of Physics and Applied Physics, School of Physical and Mathematical Sciences, Nanyang Technological University, Singapore 637371, Singapore*

(Received 30 April 2023; accepted 11 October 2023; published 6 November 2023)

Ant foraging is one of the most fascinating examples of cooperative behavior observed in nature. It is well studied from an entomology viewpoint, but there is currently a lack of mathematical synthesis of this phenomenon. We address this by constructing an ant foraging model that incorporates simple behavioral rules within three task groups of the ant colony during foraging (foragers, transporters, and followers), pheromone trails, and memory effects. The motion of an ant is modeled as a discrete correlated random walk, with a characteristic zigzag path that is congruent with experimental data. We simulate the foraging cycle, which consists of ants searching for food, transporting food, and depositing chemical trails to recruit and orient more ants (*en masse*) to the food source. This allows us to gain insights into the basic mechanism of the cooperative interactions between ants and the dynamical division of labor within an ant colony during foraging to achieve optimal efficiency. We observe a disorder-order phase transition from the start to the end of a foraging process, signaling collective motion at the population level. Finally, we present a set of time delay ODEs that corroborates with numerical simulations.

DOI: [10.1103/PhysRevE.108.054306](https://doi.org/10.1103/PhysRevE.108.054306)**I. INTRODUCTION**

Ants have been an integral part of terrestrial ecosystems since they appeared about 100 million years ago. There are about 10^{16} ants living on earth today, and they perform many crucial functions, such as aeration of soil, dispersal of seeds, and decomposition of nutrients that facilitate the creation and maintenance of biomes and habitats around the globe [1–3]. They have evolved to be highly diverse to better adapt to local environments and conditions, with more than 15 700 named species and subspecies [4]. Due to their ubiquity, ants have been studied extensively in the past hundred years. Ants display a plethora of fascinating behaviors, e.g., highly complex ways of communication using pheromones, division of labor via a caste system, eusociality social structure, and cooperative transport, to name a few [1,5–8].

Ants are known to perform random searches when foraging for food, leaving behind characteristic zigzag trails [9–12]. Zigzag paths are also found in a variety of walking and flying insects either following pheromone trails or moving up odor plumes [13]. The movement of foraging ants, or insects in general, can be described by the language of random walks [14–18]. At a small to medium timescale, ants can be modeled as persistent random walkers, i.e., correlated random walks [19–23], while at longer timescales, they are better described by Lévy walks [24–29]. A correlated random walk (CRW) is a random walk strategy where a correlation is explicitly introduced between the directions of successive steps (i.e., memory). However, the memory effects have a finite range, and beyond certain spatial and temporal scales, CRWs

typically become uncorrelated, i.e., diffusive. A previous study has proposed a necessary criterion for distinguishing true superdiffusion from correlated random walk processes [30]. On the other hand, Lévy walks are superdiffusive in nature stemming from the power-law distribution of the random walk flight length, ℓ , $p(\ell) \sim \ell^{-\mu}$. A Lévy flight forager will search intensely in a local region, and the occasional large flight steps take the forager into faraway uncharted territory. This characteristic makes Lévy processes highly useful as it improves success rate under a wide range of search scenarios in biological systems, such as collective searching, group cohesion, and encounter rate [31–34].

By working cooperatively, ants can overcome their physical limitations and complete tasks that are otherwise impossible. They exhibit what is known as collective behavior where individual ants following simple behavioral rules based on local interactions result in an organized and complex collective motion at the population level [9,35–43]. The complexity of the ant society derives from the level of local interactions between individual ants, and generally, the larger the colony size, the more advanced are the social traits [1,44–47]. In small and more “primitive” ant societies (population size $10^1 \lesssim N \lesssim 10^4$), foraging tends to be solitary and rely on a slow, individual recruitment, i.e., tandem running, where a recruiter interacts directly with one or a few individuals [48–51]. The larger and more advanced societies ($10^2 \lesssim N \lesssim 10^7$) rely on the more efficient mass recruitment, where one recruiter interacts via a chemical trail with a large number of potential recruits [35,41,52–54]. Pheromones are a chemical secreted and deposited by insects, among other creatures, for communication purposes, and ants are known to use multiple pheromones with varying chemical compositions, strengths, and lasting times to inform other ants about the quality of

^{*}eehou@ntu.edu.sg

a food source [53,55,56]. This prevents recruiting too many ants to a single food source and thus reduce overall food intake for the ant colony. Between these two limits, one finds the different types of recruitment such as leader scouting, group recruitment, etc. The transition from tandem running to mass recruitment is characterized by an increasing number of nest mates that react to the recruiters' signals and is highly correlated with an increase in colony size [46,47].

Intriguingly, there is no central control in an ant colony that regulates the number of workers engaged in each task. Instead, ants will dynamically switch tasks through local interactions, e.g., when more food is available, more foragers may choose to work to collect food. Typically, ants can do a certain number of interdependent tasks and the numbers engaged in one task depend on numbers engaged in another. This dynamic allocation of tasks depends on the rate of local interactions between ants and the information shared via these interactions, and controls how well a colony reacts to changes in environment conditions and has direct implications on a colony's long-term survivability [5,6,43]. The better the allocation of tasks, the more efficient is the ant colony, and the larger population it can support. The larger and more advanced ant colonies evolved caste system where there is a clear division of labor, resulting in optimal efficiency [1,57,58].

Despite the wealth of empirical evidence on foraging behavior in ants, there is currently a lack of quantitative synthesis of how ants work together to forage food. In this paper, we hope to address this gap in research knowledge by proposing a model that incorporates ant movement, foraging strategy, task allocation, pheromone trail, and memory effects in a unified manner. The paper is organized as follows. In Sec. II we discuss three discrete random walk models for modeling ant movement. The spatial and temporal statistics of the proposed ant movement models are investigated in Sec. III. In Sec. IV a numerical model consisting of three task groups within an ant colony, foragers, transporters, and followers, is described that models the dynamic process of task allocation in an ant colony. In Sec. V we present a ODE model, analogous to the SIR epidemic model, to describe the time evolution of the three task groups of the ant colony. In Sec. VI we summarize the findings of our ant foraging model and conclude with some future directions. Our study sheds light on the interplay between different mechanisms that enable collective foraging in ants and bridges perspectives from myrmecology, statistical physics, dynamical systems, socioecology, and organizational behavior.

II. COMPUTATIONAL MODEL OF ANT MOVEMENT

In order to understand the implications of the types of sinuous paths that an ant may make during foraging, we model it as a discrete random walk in two dimensions. The turning angles between steps have been shown to be important in the efficiency of the foraging process [59,60], a feature which we will investigate as well. As we are primarily interested in foraging in a local region, i.e., short to medium timescales, we will consider only correlated random walk in this work [15,19]. The path of an ant is discretized into a series of t temporal steps with $t + 1$ vertices, $\{\mathbf{r}_0, \mathbf{r}_1, \dots, \mathbf{r}_t\}$, separated by a fixed step size $|\mathbf{r}_i - \mathbf{r}_{i-1}| = \ell$, and turning angles

$\theta_i \in [-\Theta, \Theta]$ for $i = 1, 2, \dots, t$, as shown in Fig. 1(b). Two random walk step vectors differ only in their angular directions. The turning angles θ_i between successive step vectors \mathbf{r}_i and \mathbf{r}_{i+1} are assumed to be i.i.d. random variables consisting of two independent processes, $\theta_i = U_i V_i$, where $U_i = \pm 1$ is a random variable that determines the probability of turning left or right, V_i is a random variable that is uniformly distributed between $[0, \Theta]$, and Θ is the maximal directional deviation, an adjustable parameter.

In this work we will consider three distinct ant movement by changing the probabilities of turning left or right at each time step. In the simplest case, which we term a simple random walk (SRW), the turns are uncorrelated from each other, i.e., memoryless, and

$$P(U_i = +1) = p, \quad \text{if ant turns left (L),} \quad (1)$$

$$P(U_i = -1) = 1 - p, \quad \text{if ant turns right (R),} \quad (2)$$

which is invariant from step to step. For our work, we will consider only an unbiased simple random walk, i.e., Brownian random walkers, in which case we set $p = 1/2$.

Since foraging ants have a distinctive zigzag path [12,13] as illustrated in Fig. 1(a), we expect successive step orientations to be anticorrelated, i.e., a right turn is more likely to be followed by a left turn. Within our formalism, we can add correlations to the random walk by modifying the generating function of U . For the simplest case of CRW, which is a first-order Markov chain [15], the probability distribution for the $(i + 1)$ -th step depends only on the i th step. The chain is temporally homogeneous, i.e., $P(U_2 = u_2 | U_1 = u_1) = P(U_{i+1} = u_2 | U_i = u_1)$ where $u_i = \pm 1$, with transition probabilities

$$P(U_{i+1} = \pm 1 | U_i = \pm 1) = \gamma, \quad (3)$$

$$P(U_{i+1} = \pm 1 | U_i = \mp 1) = 1 - \gamma, \quad (4)$$

where $0 < \gamma \leq 1/2$ is a parameter that controls how anticorrelated the current step is with the previous step. The evolution of the probabilities to turn left or right for the first few time steps is shown in Fig. 1(c), with initial conditions given by $P(U_1 = \pm 1) = 1/2$. In this work, we will term this type of movement the first-order correlated random walk (FCRW). As $\gamma \rightarrow 1/2$, the statistics of the FCRW becomes identical to the SRW defined earlier.

CRW can become more complex by increasing its memory, in which case the probability distribution for the $(i + 1)$ -th step will depend not only on the i th step, but the $(i - 1)$ -th step, and so on, $P(U_{i+1} = u_{i+1} | U_1 = u_1, U_2 = u_2, \dots, U_i = u_i)$. This changes the statistics of the random walk and leads to nontrivial asymptotic behavior [14,21,22]. In order to increase the amount of anticorrelation between successive steps, we propose a long-range correlated random walk that we term the zigzag walk (ZW), with the following sets of rules: If $U_i = \pm 1$ and $P(U_i = \pm 1) \geq 1/2$, then

$$P(U_{i+1} = \pm 1) = \gamma, \quad P(U_{i+1} = \mp 1) = 1 - \gamma. \quad (5)$$

If $U_i = \pm 1$ and $P(U_i = \pm 1) < 1/2$, then

$$P(U_{i+1} = \pm 1) = \gamma P(U_i = \pm 1), \quad (6)$$

$$P(U_{i+1} = \mp 1) = 1 - \gamma P(U_i = \pm 1). \quad (7)$$

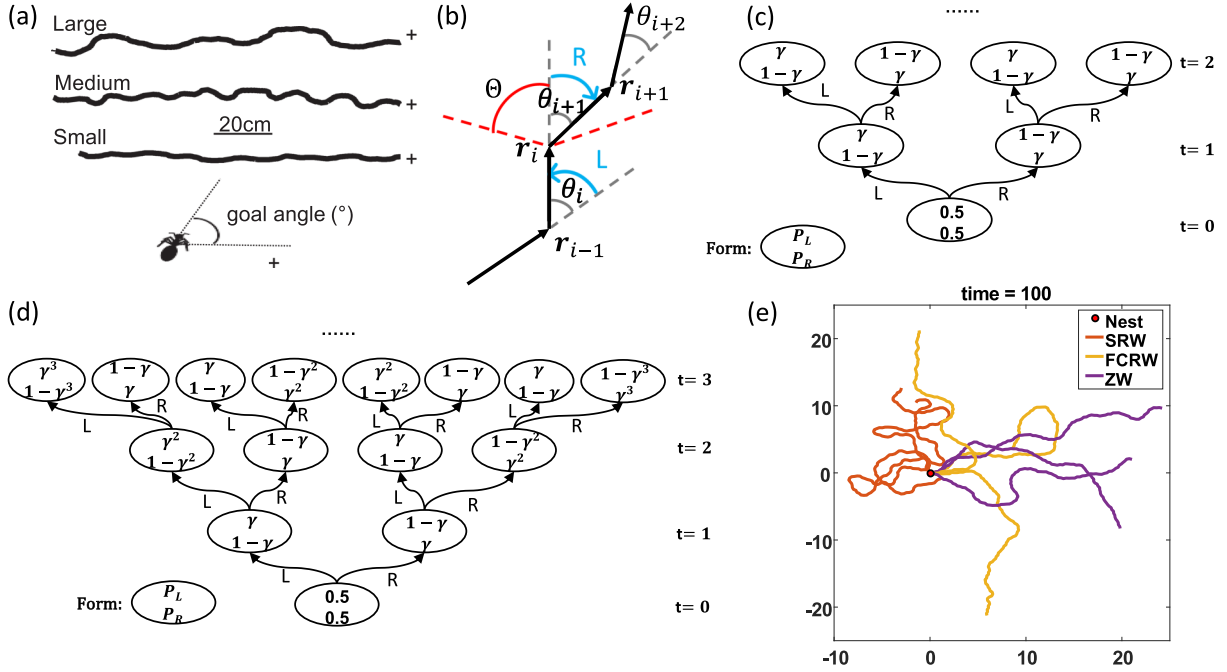


FIG. 1. Modeling ant movement as a discrete random walk. (a) Distinctive zigzag ant paths of different amplitudes. Image is courtesy of Ref. [11]. (b) A discrete ant path consist of t temporal steps with $t + 1$ vertices, $\{\mathbf{r}_0, \mathbf{r}_1, \dots, \mathbf{r}_t\}$, separated by a fixed step size $|\mathbf{r}_i - \mathbf{r}_{i-1}| = \ell$ and turning angles $\theta_i \in [-\Theta, \Theta]$. Negative θ_i indicates left turn (L), while positive θ_i indicates right turn (R). (c) A tree diagram showing the turning probability $P_{L/R} = P(T_i = \pm 1)$ of the first three time steps of the first-order correlated random walk (FCRW). Note that $0 \leq \gamma \leq 0.5$. (d) A tree diagram showing the turning probability $P_{L/R}$ of the first four time steps of the zigzag walk (ZW). (e) Two-dimensional discrete random walks of 20 time steps for SRW (red), FCRW (yellow), and ZW (purple), three sample trails for each type of random walk. There is noticeable directional persistence in FCRW and ZW.

The probabilities to turn left or right for the first few steps are shown in Fig. 1(d). The probability of an ant making k consecutive turns in a single direction is γ^k , which quickly approaches 0 as k increases. This leads to a correlated random walk with finite memory that penalizes consecutive turns in the same direction heavily [21], i.e., ZW promotes turn sequences with alternating left and right turns such as $\dots \text{LRLRLRLR} \dots$ and suppresses sequences such as $\dots \text{RRRRLLLL} \dots$. Some sample paths generated using SRW, FCRW, and ZW are shown in Fig. 1(e), and it is evident that FCRW and ZW demonstrate significant directional persistence.

In our simulations, ants are represented by self-propelled point dots with a constant speed of $v_0 = 0.6$ unit length per unit time with an interaction-vision range of $\delta = 0.6$ unit length. This relative scale of the ant size, speed, and interaction-vision range is based on a previous study on the visual capabilities of ants [61]. For each simulation, the ants can move freely in two-dimensional (2D) real space, \mathbb{R}^2 , according to the one of the ant movement models: SRW, FCRW, or ZW. At each temporal step, the position of every ant is updated based on the chosen ant movement model.

III. SPATIAL AND TEMPORAL STATISTICS OF ANT MOVEMENT

By looking at the spatial and temporal statistics of the random walkers, we can better understand the characteristics of the sinuous trails produced by the different ant movement

models. We generated 2D ant trails using FCRW and ZW and compared them with the time series data collected by Lent *et al.* [12]. The case of SRW is not considered as it does not conform with empirical data. Since the ants in our simulations do not have a goal, the direction of motion is defined by the direction of the line that cuts the sinuous ant trail into two equal parts. The goal angle, ζ_i , defined relative to the direction of motion, is the running total of the turning angles θ_i :

$$\zeta_i = \sum_{k=0}^i \theta_k. \quad (8)$$

The amplitude of the CRWs can be varied by the anticorrelation parameter γ : larger γ leads to bigger amplitudes [see Figs. 1(a) and 2]. The variations in the goal angle is approximately sinusoidal with a period that increases with γ . Qualitatively, we see that both FCRW and ZW produce paths that are zigzag in nature and reach a high similarity with experimental results of the foraging paths of wood ants [12].

The mean resultant length of a 2D random walk is given by

$$\rho = \langle \cos \theta \rangle = \int_{-\Theta}^{\Theta} d\theta f(\theta) \cos \theta, \quad (9)$$

where $f(\theta)$ is the probability density function (pdf) for the turning angles [14]. The value of the mean resultant length reflects the amount of directional persistence of a random walk. For a simple random walk where $\Theta = \pi$ and $f(\theta) = 1/2\pi$, we find that $\rho = 0$. In the extreme case, when the pdf is a Dirac δ function, i.e., $f(\theta) = \delta(\theta)$, the resulting walk is a

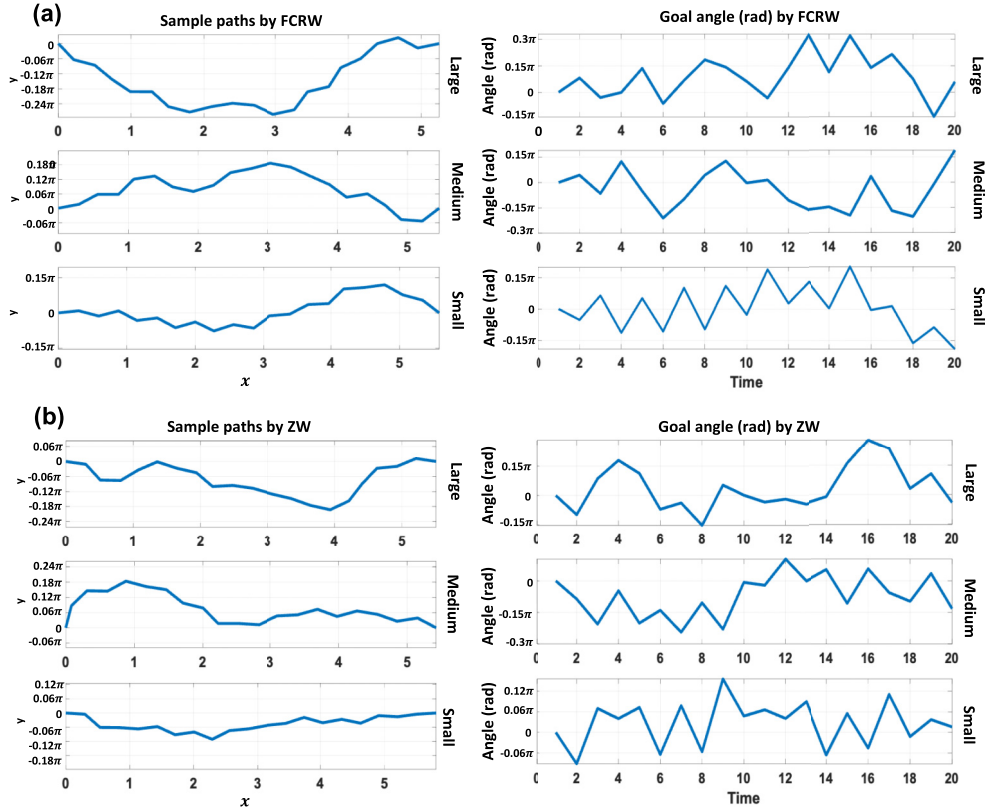


FIG. 2. Temporal statistics of ant movement. (a) Sample sinuous ant trails of 20 time steps generated by FCRW (left panel) and the corresponding goal angle (right panel) as a function of time step for $\Theta = 60^\circ$ and $\gamma = 0.45$ for top row (large), 0.25 for second row (medium), and 0.1 for bottom row (small). (b) Sample ant trails of 20 time steps (left) generated by ZW and the corresponding goal angle (right) as a function of time step for $\Theta = 60^\circ$ and $\gamma = 0.49$ for top row (large), 0.3 for second row (medium), and 0.1 for bottom row (small).

straight line and ballistic in nature, with $\rho = 1$. For a given set of parameter values, Θ and γ , we find that the mean resultant lengths for FCRW and ZW are almost identical. As seen from Fig. 3(a), ρ does not appear to depend on γ , i.e., $\partial\rho/\partial\gamma = 0$, and has a quadratic dependence on the Θ given by

$$\rho(\Theta) = 1 - 3.9e^{-4}\Theta - 4.1e^{-5}\Theta^2, \quad (10)$$

which approaches 1 as $\Theta \rightarrow 0$ as expected.

All CRWs possess a characteristic timescale τ associated with the exponentially decaying correlations present in Markov processes. The dimensionless two-point correlation function of a random walk is defined by

$$C(|j - i|) = \frac{\langle \mathbf{r}_j \cdot \mathbf{r}_i \rangle}{\langle r_j r_i \rangle} = e^{-|j-i|/\tau}, \quad (11)$$

where i, j are integer indices representing time step and $r_j = \|\mathbf{r}_j\|$ is the magnitude of the position vector \mathbf{r}_j [14]. The correlation functions for FCRW and ZW are shown in Fig. 3(b), where we find that the correlation time of ZW to be larger than that of FCRW for any given Θ and γ , $\tau_{ZW} > \tau_{FCRW}$, which is expected since ZW is a CRW with longer memory than FCRW.

A random walker is known to return multiple times to previously visited territories, a phenomenon known as oversampling [14]. The territory covered by a random walker is a well-studied problem dating back to the great mathematician G. Pólya, who established the mathematical framework of

studying random walks on a lattice [62,63]. Let $S_1(t)$ be the number of distinct sites visited by a single (Brownian) random walker in a t -steps walk. $S_1(t)$ provides a direct measure of the territory covered by a single foraging ant. In this work, we will consider only the case of spatial dimension $d = 2$. The expected value of $S_1(t)$, i.e., $\langle S_1(t) \rangle$, is discussed by Dvoretzky and Erdős [62–64], who found that

$$\langle S_1(t) \rangle \sim \frac{\pi t}{\log t} \quad \text{as } t \rightarrow \infty. \quad (12)$$

In writing the tilde (\sim), we emphasize only the scaling relation and ignore all numerical coefficients.

Larralde *et al.* addressed the problem of evaluating the number of distinct sites covered by a set of N -independent (Brownian) random walkers in d dimensions, $\langle S_N(t) \rangle$, initially placed at the origin [65–67]. When there are N random walkers searching for food collectively, not only must each forager not oversample the sites it has previously visited, it also must not oversample the sites visited by the other $N - 1$ walkers. $\langle S_N(t) \rangle$ is a useful concept in ecology, chemical reactions, and spreading phenomena and in situations where there are multiple foragers in the system, such as the ant colony studied in [25]. It is evident that $\langle S_N(t) \rangle$ is not related simply to $\langle S_1(t) \rangle$. The asymptotic form of $\langle S_N(t) \rangle$ for $N \gg 1$ depends on the dimension of the lattice, d , as well as the timescale of foraging, with three distinct time regimes. For $d = 2$ and

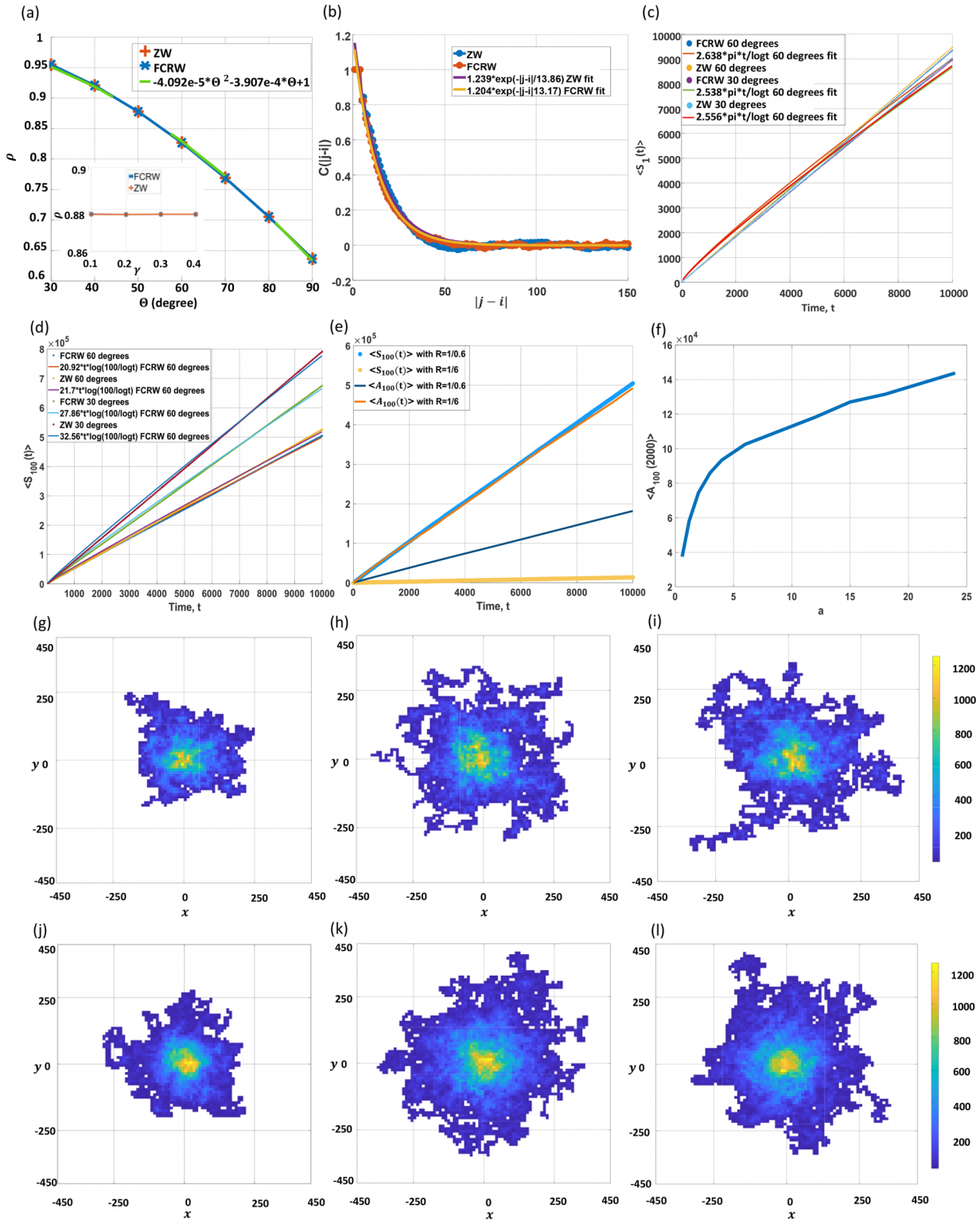


FIG. 3. Spatial statistics of ant movement. (a) The mean resultant length, ρ , for FCRW and ZW is almost identical for any set of Θ and γ . ρ has a quadratic dependence on Θ . Inset: ρ does not depend on γ . (b) The dimensionless two-point correlation function of a random walk for FCRW and ZW. $\tau_{ZW} = 13.86$ and $\tau_{FCRW} = 13.17$. $\langle S_n(t) \rangle$ is the average number of distinct sites visited by i random walkers in a t -steps walk, where $n = 1$ or N [see Eqs. (12) and (13)]. Plot of $\langle S_n(t) \rangle$ and its corresponding fitted curve for FCRW and ZW under different parameter values: (c) $\langle S_1(t) \rangle$ (average of 30 simulations), (d) $\langle S_{50}(t) \rangle$ (average of 15 simulations), and (e) $\langle S_{100}(t) \rangle$ (average of 15 simulations). (f) Plot of $\langle S_{100}(t) \rangle$ and $\langle A_{100}(t) \rangle$ [see Eq. (14)] for ZW with $\Theta = 60^\circ$ and $\gamma = 0.2$ under different resolution R . Set of visited sites, $S_N(t)$, as a function of time, t , for $\Theta = 60^\circ$, $\gamma = 0.2$, and $R = 1/6$: (g) SRW ($N = 50$), (h) FCRW ($N = 50$), (i) ZW ($N = 50$), (j) SRW ($N = 100$), (k) FCRW ($N = 100$), and (l) ZW ($N = 100$).

$\log N < t < e^N$, it is known that

$$\langle S_N(t) \rangle \sim t \log \left(\frac{N}{\log t} \right). \quad (13)$$

At very long times ($t > e^N$), the random walkers are so sparse that they can be treated independently, in which case, $\langle S_N(t) \rangle \sim N \langle S_1(t) \rangle$.

At timescales comparable to the correlation time τ , $\langle S_1(t) \rangle$ and $\langle S_N(t) \rangle$ depend on the specific details of the CRW. At timescales much larger than the correlation time, i.e., $t \gg \tau$, all CRWs will appear Brownian, i.e., uncorrelated. Hence, we expect the general scaling behavior of $\langle S_1(t) \rangle$ and $\langle S_N(t) \rangle$ for CRWs to be given by Eqs. (12) and (13), respectively. For a persistent random walker in two dimensions that cannot reverse direction, it has been shown that mean number of distinct sites visited scales as Eq. (12) as expected [68].

To facilitate the calculation of $\langle S_1(t) \rangle$ and $\langle S_N(t) \rangle$, we tile our 2D space by regular grid squares of length a , including the square centered at the origin, with the center of each square taken as a lattice site. Each time an ant wanders anywhere inside a grid square, we count the associated lattice site as visited. For the case of N ants, new territory is counted only when a site is visited for the first time. It is useful to define the resolution, R , as the inverse of the lattice spacing a . The results of $\langle S_1(t) \rangle$ and $\langle S_N(t) \rangle$ are shown in Figs. 3(c), 3(d), and 3(e) for $\Theta = 30^\circ$ or 60° , $\gamma = 0.2$, and $R = 5/3$. The figures provide intuitive views of how foraging ants explore area around their starting spot. The numerical data can be fitted by either Eqs. (12) or (13), and generally, we find that the proportionality constant increases with decreasing Θ . For most of the parameter values tested, we find that ZW results in a slightly larger number of distinct sites visited, implying a higher foraging efficiency as compared to FCRW.

The mean total foraging area is given by [69]

$$\langle A_i(t) \rangle = a^2 \langle S_i(t) \rangle, \quad (14)$$

where $n = 1$ or N . As we increase the resolution, the number of distinct sites visited $S_i(t)$ will increase as shown in Fig. 3(f). Due to the vision range of the ant as well as the size of the ant, we introduce a lower bound to the length of the square, $a \geq 0.5$. We find that this allows for a sensible interpretation of the foraging area.

Figures 3(g) to 3(l) show the geometry of the set of visited sites, $S_N(t)$, from our numerical simulations for the different ant movement models with $\Theta = 60^\circ$, $\gamma = 0.2$, and $R = 1/6$. At very small times, there are more ants than accessible sites, and the boundary of the set $S_N(t)$ grows isotropically in a disklike shape with relatively smooth boundary. As the ants forage further from the origin, eventually the number of accessible sites outgrows the number of ants, N , and not all the accessible sites are visited. At longer times, the ants become more isolated and the boundary of the visited set becomes progressively rough with noticeable fractal patterns [65,66].

IV. DISORDER-ORDER TRANSITION IN FORAGING ANTS

We consider the dynamics of the division of labor within an ant colony during foraging using mass recruitment, i.e., pheromone trails, and investigate the effects of cooperative interactions between foraging ants and how these may influence

the emergent behavior observed in such systems [5,55,70]. Organisms such as social insects typically exhibit some form of “order-disorder” transitions whereby aggregations of insects go from an initial “disordered” state to a final coordinated collective state such as foraging transition in the Pharaoh’s ant in [71], chaotic to periodic transitions in ants [39], and density-dependent transition in [72,73]. Our ant colony is assumed to be homogeneous, with no caste system, i.e., identical ants. To this end, we classify ants into three task groups, i.e., population compartments, depending on their roles, namely, foragers, transporters, and followers [6,39,43]. Foragers are responsible for the scouting of food; transporters, aside from transporting food, deposit pheromone to recruit and guide other ants *en masse* to the food source; followers follow pheromone trail to the food source. During the the course of a foraging cycle, the role of individual ants will evolve based on local behavioral rules: A forager can turn into a transporter if it discovers a food source, or it can become a follower if it encounters a pheromone trail. A transporter will turn into follower after it deposits food at the nest, while a follower will turn into a transporter once it reaches the food source. Eventually, all the ants are either followers or transporters moving along the pheromone trail.

Foraging ants can memorize the location of their nest using landmarks and path integration and can therefore traverse home from the food source with little difficulty [37,54,55,74]. In fact, ants need to memorize only some parts of their spatial movement to be able to retrace their way back to the nest [51,75,76]. Consider the sinuous path of a foraging ant given by $\Gamma = \{\mathbf{x}_0, \mathbf{x}_1, \dots, \mathbf{x}_l\}$, where \mathbf{x}_0 and \mathbf{x}_l are the locations of the nest and the food source, respectively. In this work we assume that each ant only memorizes a third of its positional information over time, including the locations of the nest and the food source, i.e., $\Gamma_1 = \Omega(\Gamma) = \{\mathbf{x}_0, \mathbf{x}_3, \dots, \mathbf{x}_k, \mathbf{x}_{k+3}, \dots, \mathbf{x}_l\}$. The resultant route Γ_1 is a simpler path with less meandering, and hence the transporter ant, through retracing its steps, can return to the nest in a shorter time.

Transporters will deposit a pheromone to transmit information to other foraging ants about the presence of the food source. In our study, we only consider a single kind of pheromone because there is only one limitless food source and the route between the nest and the food source is simple. The density of the pheromone reflects the the credibility of a path: when encountering multiple pheromone trails, ants will choose to move along the one with the largest concentration of pheromone [53–55]. The pheromone trails will shift with time, eventually stabilizing into a single optimal path between the nest and the food source, which is a straight line in our setup.

We can understand why the pheromone trails in our model are self-optimizing as follows: The operation Ω defined above is an example of coarse graining, which is a procedure that removes less relevant features from a physical system [77]. If we repeat this coarse-graining operation a sufficiently large number of times on any path Γ , eventually we will be left with a straight path connecting the nest and the food source. In reality, the picture is more complicated as there are multiple pheromone trails from different ants that interact with one another. There is a fine interplay between the coarse-graining

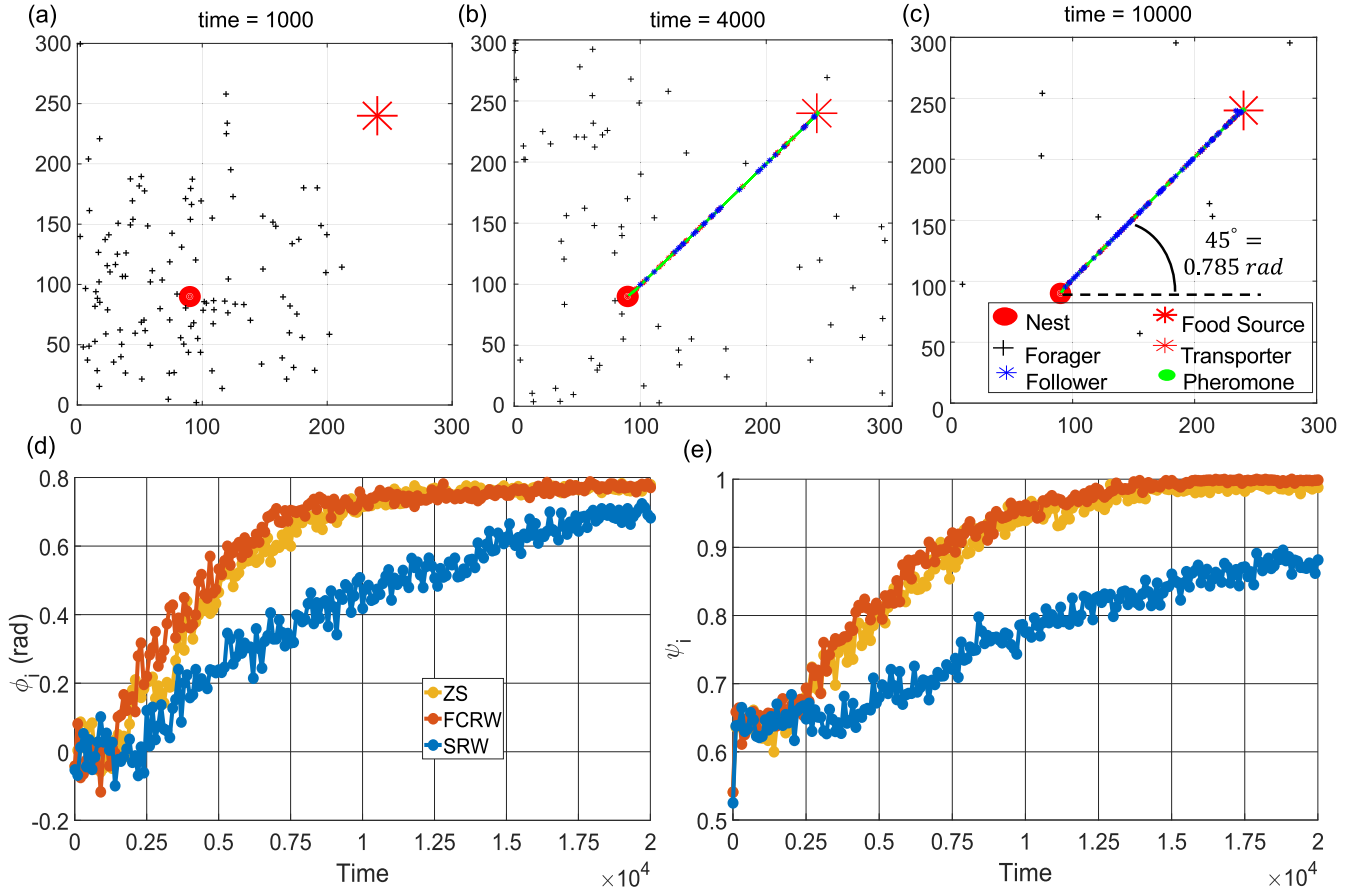


FIG. 4. Disorder-order phase transition in foraging ants. We simulate $N = 100$ ants in a box with reflective boundaries. Ants can take on the role of foragers (F), transporters (T), and followers (f). At $t = 0$, ants (all foragers) leave the nest in random directions in search of food. (a) Snapshot of the position of the ants at $t = 1000$. (b) The pheromone trail between the nest and the food source is well established by $t = 4000$. (c) By $t = 10000$, most of the ants are moving along the pheromone trail as either transporters or followers between the nest and the food source. Time evolution of the (d) orientation order parameter ϕ_i [see Eq. (16)] and (e) nematic order parameter ψ_i [see Eq. (17)] from three simulations using SRW, FCRW, and ZW. Initially, the ant colony is in a disordered state, i.e., $\phi_i \approx 0$ and $\psi_i \approx 0.64$. The order parameters start to increase rapidly at around $t = 2000$ for FCRW and ZW, while the rise in SRW starts at $t = 6000$ and at a slower rate. By $t = 10000$, simulations from FCRW and ZW attain $\phi_i \approx 0.785$ and $\psi_i \approx 1$, indicating that the ant colony is in an ordered state.

effects of memory and behavioral rules from pheromone trail interactions. Eventually, the route of the transporter ant converges to a straight line for our setup, which is the optimal path to travel between the nest and the food source.

Our simulation box is a 2D area of size $A = L \times L$ ($L = 300$ unit length) with reflective boundaries, consisting of an ant nest with population $N = 100$ and an (inexhaustible) food source. The angle that the line connecting the nest and the food source makes with the horizontal axis is $\pi/4 \approx 0.785$ as seen in Fig. 4(a). This set of food foraging simulations was done with parameters set to $\gamma = 0.1$ and $\Theta = 50^\circ$.

The position of the α th ant at time step i during foraging is given by $\mathbf{x}_i^{(\alpha)} = (x_i^{(\alpha)}, y_i^{(\alpha)})$, where $i = 0, 1, \dots, t$ and $\alpha = 1, 2, \dots, N$. The orientation angle of the α th ant at the i th step is defined by

$$\phi_i^{(\alpha)} = \arctan \left(\frac{y_i^{(\alpha)} - y_{i-1}^{(\alpha)}}{x_i^{(\alpha)} - x_{i-1}^{(\alpha)}} \right). \quad (15)$$

The orientation angle is defined over the range $(-\pi/2, \pi/2)$ as we do not distinguish an ant that is moving in the $\hat{\mathbf{v}}$ direction from another that is moving in the $-\hat{\mathbf{v}}$ direction. This implies an equivalence in the velocity $\hat{\mathbf{v}} \equiv -\hat{\mathbf{v}}$. The orientational order parameter, which is the average orientation angle of the whole ant colony at time step i , is given by

$$\phi_i = \frac{1}{N} \sum_{\alpha=1}^N \phi_i^{(\alpha)}. \quad (16)$$

At the start of the foraging process, all the ants are foragers and they set off in different random directions from the nest in search of food. The orientational order parameter ϕ_i fluctuates about zero, indicating that the ant colony is in a disordered state. In the early stages of the foraging process, only a few ants are able to locate the food source. When a forager locates a food source, it becomes a transporter and starts bringing food back to the nest. Note that the physical process of transportation of the food is not in the scope of this research [8],

and only the movement of ants is considered. As more ants discover the position of the food source, a pheromone trail begins to form which helps to spread spatial information about the food source. Over time, many ants begin to move along an increasingly optimized and well-defined pheromone path and the orientation order parameter ϕ_i slowly approaches $\pi/4$ as expected. Overall, we observe a disorder-order transition from an initial random state $\phi_i \approx 0$ to an emergent collective motion where $\phi_i \approx \pi/4$. This transition happens much faster for simulations ran using FCRW and ZW as seen from Fig. 4(d), generally reflecting the higher efficiency of foraging and better division of labor for both FCRW and ZW.

Another useful order parameter to consider is the 2D nematic order parameter ψ_i , which is the average normalized velocity of the ant colony of N ants at time step i ($i = 0, 1, \dots, t$), with the equivalence in velocity $\hat{v} \equiv -\hat{v}$, i.e., mathematically equivalent to the director of a nematic liquid crystal [78]:

$$\psi_i = \frac{1}{Nv_0} \left| \sum_{\alpha=1}^N \hat{v}_i^{(\alpha)} \right| = \frac{1}{N} \left| \sum_{\alpha=1}^N \hat{v}_i^{(\alpha)} \right|. \quad (17)$$

The order parameter space is \mathbb{RP}^1 where the antipodal points of the unit circle are identified [77]. Note that $\hat{v}_i^{(\alpha)} = \hat{v}_{i,x}^{(\alpha)} \mathbf{i} + \hat{v}_{i,y}^{(\alpha)} \mathbf{j}$.

In the early stages of foraging, the average normalized velocity ψ_i fluctuates about $2/\pi \approx 0.64$, indicating that the ant colony is in a disordered state. Since the angular distribution of the ants is roughly uniform at the start, we find that

$$\frac{1}{N} \sum_{\alpha=1}^N \hat{v}_{i,x}^{(\alpha)} \approx \frac{1}{\pi} \int_{-\pi/2}^{\pi/2} \sin \theta d\theta = 0, \quad (18)$$

$$\frac{1}{N} \sum_{\alpha=1}^N \hat{v}_{i,y}^{(\alpha)} \approx \frac{1}{\pi} \int_{-\pi/2}^{\pi/2} \cos \theta d\theta = \frac{2}{\pi}, \quad (19)$$

and hence, the nematic order parameter ψ_i is $2/\pi \approx 0.64$. The nematic order parameter ψ_i starts to increase shortly after the first ant locates the food source. After a pheromone trail between the nest and food source is established, most ants are moving along this route transporting food. This orderliness is reflected in the average normalized velocity which asymptotes to one over time, $\psi_i \rightarrow 1$ as i grows, indicating the emergence of an ordered collective motion at the population level [39,71]. As seen from Fig. 4(e), ψ_i rises significantly faster in simulations with ants performing either FCRW or ZW as compared to SRW, consistent with what we saw in ϕ_i .

From the time evolution of the orientation order parameter ϕ_i and the nematic order parameter ψ_i , one can observe the disorder-order transition in the motion of the ants. The growth in the order parameters is due to the discovery of the food source by the first ant and the subsequent formation of a pheromone trail. The time at which the order parameter changes nontrivially is commonly known as the first-passage time (FPT), or first hitting time, in stochastic processes [22,79,80], and indicates when a stochastic event occurs for the first time. Due to the random nature of this time,

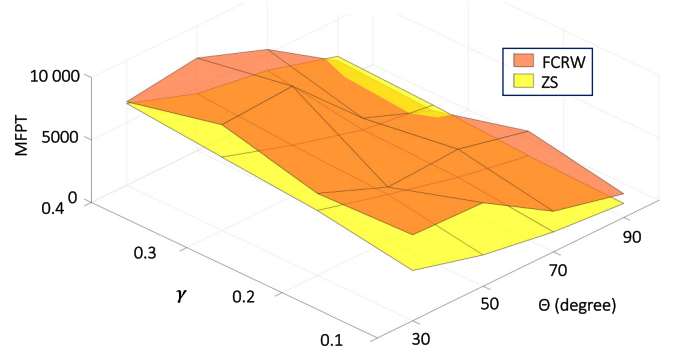


FIG. 5. Mean first-passage time (MFPT) as a function of the maximal directional deviation, Θ , and the anticorrelation parameter, γ . MFPT is defined as the average time an ant colony first finds the food source; each data point (vertex of surface) is the average from 30 simulations.

it is more meaningful to look at the mean first-passage time (MFPT) instead, which in our case, is the average time taken for the first ant from the colony to find the food source.

We calculated the MFPT for both FCRW and ZW at different combinations of the maximal directional deviation, Θ , and the anticorrelation parameter, γ , by averaging the FPT from 30 simulations. In our study, we set $\Theta \in [\pi/6, \pi/2]$ (radian) and $\gamma \in [1/10, 1/2]$. When Θ is small, e.g., $\Theta = \pi/6$, an ant can turn by only a small angle from step to step and the resultant ant path is relatively straight. As we increase Θ , e.g., $\Theta = \pi/2$, the ant can rotate significantly and the path becomes sinuous. γ controls how biased the probabilities of turning are, from totally unbiased at $\gamma = 1/2$ to extremely biased at $\gamma = 1/10$. The full results for the MFPT is shown in Fig. 5. SRW is not shown because it performs significantly worse than FCRW and ZW.

Intuitively, ZW has a smaller MFPT than FCRW for most of the range of parameters analyzed in our study, suggesting the superiority of ZW over FCRW for food foraging. The long-range correlations of ZW result in paths that are less sinuous and reduce the issue of oversampling. The difference between the two random walks is more apparent when the turn parameter γ is large, as oversampling becomes increasingly problematic, particularly for FCRW. Under these conditions, FCRW becomes similar to SRW, while ZW still maintains characteristics of a zigzag walk with a good degree of directional persistence.

V. DYNAMICAL MODEL FOR ANT FORAGING

Ordinary differential equations (ODEs) are used to model the dynamics of a wide variety of systems, from the epidemic spreading to the regulations of phenotypes circuits [81–83]. These theoretical models provide an intuitive and insightful way to understand the evolution of complex systems, and offer predictions of different outcomes as the parameters are varied. Here we propose a simple theoretical model to understand the division of labor during ant foraging [55,84], analogous to the famous SIR epidemic model, which tracks the number

of ants in each of three groups: foragers (F), transporters (T), and followers (f), given by

$$\frac{dF(t)}{dt} = - \underbrace{AF(t)H(t-t_1)}_{F \text{ to } T} - \underbrace{B(1 - e^{-\frac{T(t)}{T_0}})F(t)}_{F \text{ to } f}, \quad (20)$$

$$\frac{dT(t)}{dt} = \underbrace{AF(t)H(t-t_1)}_{F \text{ to } T} + \underbrace{D(1 - e^{-\frac{f(t-t_0)}{E}})}_{f \text{ to } T} - \underbrace{C(1 - e^{-\frac{T(t-t_0)}{E}})}_{T \text{ to } f}, \quad (21)$$

$$\frac{df(t)}{dt} = \underbrace{B(1 - e^{-\frac{T(t)}{T_0}})F(t)}_{F \text{ to } f} + \underbrace{C(1 - e^{-\frac{T(t-t_0)}{E}})}_{T \text{ to } f} - \underbrace{D(1 - e^{-\frac{f(t-t_0)}{E}})}_{f \text{ to } T}, \quad (22)$$

where $H(t - t_1)$ is the Heaviside step function, t_1 is the time it takes for the first ant to find the food source, i.e., the first-passage time, T_0 is the average number of transporters needed to form a pheromone path, t_0 is the average commute time between the food source and the nest, A is the probability of foragers finding the food source, B is the probability of foragers finding a pheromone trail, C is the average rate at which transporters turn into followers, D is the average rate at which followers turn into transporters, and E is a number that reflects the effects of saturation for transporters and followers [Fig. 6(a)].

Initially, all the ants in the colony are foragers: $F(0) = N$, $T(0) = 0$, and $f(0) = 0$, and this continues until $t = t_1$. This is enforced by the presence of the Heaviside step function. After $t \geq t_1$, F , T , and f start to evolve with time but overall, the total ant population is time invariant, i.e., $F(t) + T(t) + f(t) = N$. Our ant model has no probabilistic component, except for the assumption that the population is large enough so that transitions based on average rates can be used. A forager can turn into either a transporter once it finds the food source at a constant rate of $AF(t)$ or a follower after finding the pheromone at a rate $B(1 - e^{-T(t)/T_0})F(t)$. The transition rate into follower will asymptote to $BF(t)$ as $T(t)$ becomes large because even though pheromone could accumulate infinitely in our simulations, most of it is confined to a small region between the nest and the food source, and hence the chance of a forager finding the pheromone trail is necessarily bounded. A transporter can turn into follower at a rate of $C(1 - e^{-T(t-t_0)/E})$ and the reverse rate is $D(1 - e^{-f(t-t_0)/E})$. These terms provide a self-regulatory negative feedback loop to the population of transporters and followers [40,70].

The time lag of t_0 reflects the time to commute between the food source and the nest. ODEs with time lag are known as time delay ordinary differential equations (TDODEs) and are frequently used in biomedical science and engineering [85]. Figure 6(b) reveals excellent agreement between the deterministic ODE model and the numerical simulation, which is stochastic in nature. The trajectories from the stochastic numerical simulation are continuous but nondifferentiable, while the solutions to the set of ODEs are smooth and differentiable. A new set of ODE parameters is required to fit each realization of the numerical simulation. The number of foragers

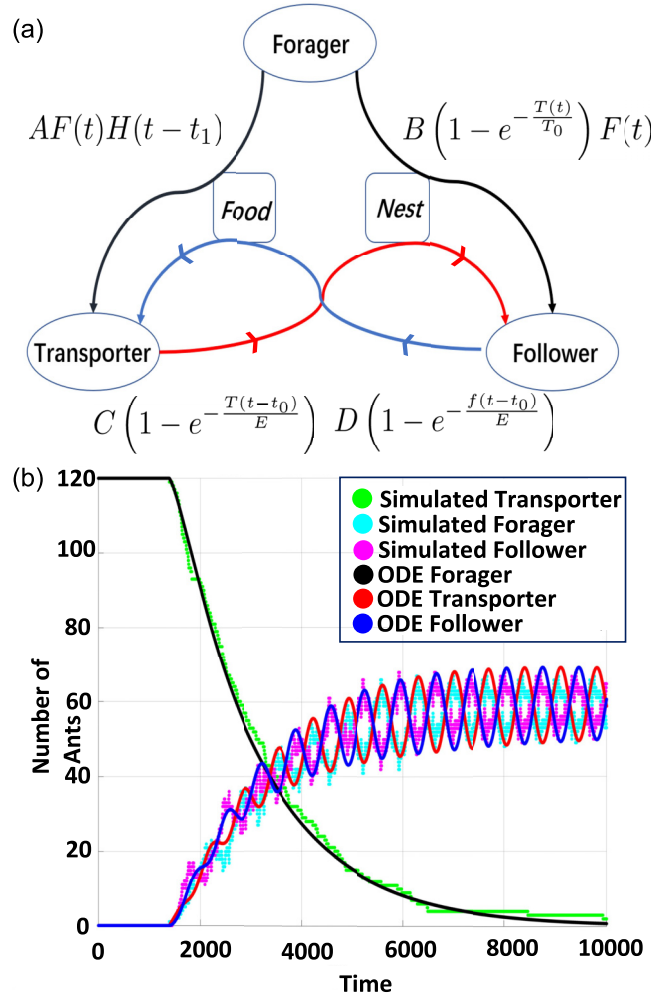


FIG. 6. A simple model of ant foraging. (a) Three task groups in our model: foragers (F), transporters (T), and followers (f). (b) One realization of the numerical model (F = cyan, T = green, and f = magenta), which is stochastic in nature, is shown. Our deterministic ODE model (F = black, T = red, and f = blue) can fit the main qualitative features of the numerical simulation.

decreases monotonically from $N = 120$ to zero as foragers are continuously converted into either transporter or follower ($F(\infty) \approx 0$). Once a pheromone trail is established, most ants are moving along this route transporting food, alternating roles between transporter and follower, and generally reflecting the ordered collective motion at the population level. The trajectories of T and f grow with time and asymptote to a value of approximately $N/2 = 60$, and we observe that $T(\infty) + f(\infty) \approx N$.

The small-amplitude modulations in the trajectory of T and f are roughly the same size and out of phase with each other, with the amplitude and period controlled by the model parameters C , D , and E . As the population of T increases, the rate of transition out of T increases correspondingly until dT/dt eventually becomes negative and T starts to drop. On the other hand, as f decreases, the rate of transition out of f decreases until df/dt eventually becomes positive, at which point f starts to grow again. The interplay between $T \rightarrow f$ and $f \rightarrow T$ transitions leads to oscillatory behavior in the

population of T and f . The amplitude modulations in the numerical simulation stem from inhomogeneity in the spatial distribution of transporters and followers on the pheromone trail. Since the ants move at constant speed, once they stabilize their motion on the pheromone trail, their relative positions are fixed, and any spatial inhomogeneity will persist indefinitely.

VI. CONCLUSION

In this work, we investigate the foraging behavior observed in ant colonies, using a combination of mathematical and numerical techniques. To understand the significance of zigzag patterns in ant trails, we present two realistic ant movement models, FCRW and ZW, and obtain the temporal and spatial statistics of these discrete correlated random walks. We construct a realistic ant foraging model that incorporates simple behavioral rules within three task groups of the ant colony (foragers, transporters, and followers), pheromone trails, and memory effects. We simulate the foraging cycle, which consists of ants searching for food, transporting food, and depositing chemical trails to recruit and orient more ants (*en masse*) to the food source. Our analyses show that ants adopting ZW has a higher efficiency in foraging based on a

smaller mean first-passage time, faster disorder-order transition, and larger foraging area. Finally, we present a set of TDODEs, similar to the SIR epidemic model, that models the time evolution of the three task groups in an ant colony during foraging which corroborates with numerical simulations. The basic ant foraging framework introduced here can be readily extended to model more realistic factors: larger search range, random walks with reorientation events (i.e., saccade-like turns), Lévy walks, egocentric and geocentric navigation, multiple food source, multiple pheromones, trail longevity (i.e., evaporation), effects of obstacles, visual memories, effects of humidity, among others.

ACKNOWLEDGMENTS

We wish to thank H. L. Tan and H. K. Teoh for their preliminary work on this project. E.H.Y. would like to acknowledge the funding support by Nanyang Technological University under its Start Up Grant Scheme No. 04INS000175C230. We would also like to acknowledge the funding support for this project from Nanyang Technological University under the Undergraduate Research Experience on Campus (URECA) program.

-
- [1] B. Hölldobler and E. O. Wilson, *The Ants* (Springer-Verlag, Berlin Heidelberg, 1990).
 - [2] B. Hölldobler and C. J. Lumsden, Territorial strategies in ants, *Science* **210**, 732 (1980).
 - [3] B. Hölldobler and E. O. Wilson, *Journey to the Ants: A Story of Scientific Exploration* (Harvard University Press, Cambridge, 1998).
 - [4] P. Schultheiss, S. S. Nooten, R. Wang, M. K. Wong, F. Brassard, and B. Guénard, The abundance, biomass, and distribution of ants on earth, *Proc. Natl. Acad. Sci. USA* **119**, e2201550119 (2022).
 - [5] D. M. Gordon, Dynamics of task switching in harvester ants, *Anim. Behav.* **38**, 194 (1989).
 - [6] D. M. Gordon, The organization of work in social insect colonies, *Nature (London)* **380**, 121 (1996).
 - [7] B. Hölldobler and E. O. Wilson, *The Superorganism: The Beauty, Elegance, and Strangeness of Insect Societies* (W. W. Norton & Company, New York, 2009).
 - [8] O. Feinerman, I. Pinkoviezky, A. Gelblum, E. Fonio, and N. S. Gov, The physics of cooperative transport in groups of ants, *Nat. Phys.* **14**, 683 (2018).
 - [9] N. R. Franks and C. R. Fletcher, Spatial patterns in army ant foraging and migration: *Eciton burchelli* on Barro Colorado Island, Panama, *Behav. Ecol. Sociobiol.* **12**, 261 (1983).
 - [10] R. J. Vázquez, P. G. Koehler, and R. M. Pereira, Comparative quantification of trail-following behavior in pest ants, *Insects* **11**, 5 (2019).
 - [11] M. Collett, L. Chittka, and T. S. Collett, Spatial memory in insect navigation, *Curr. Biol.* **23**, R789 (2013).
 - [12] D. D. Lent, P. Graham, and T. S. Collett, Phase-dependent visual control of the zigzag paths of navigating wood ants, *Curr. Biol.* **23**, 2393 (2013).
 - [13] T. S. Collett, D. D. Lent, and P. Graham, Scene perception and the visual control of travel direction in navigating wood ants, *Philos. Trans. R. Soc., B* **369**, 20130035 (2014).
 - [14] G. M. Viswanathan, M. G. Da Luz, E. P. Raposo, and H. E. Stanley, *The Physics of Foraging: An Introduction to Random Searches and Biological Encounters* (Cambridge University Press, New York, 2011).
 - [15] P. Kareiva and N. Shigesada, Analyzing insect movement as a correlated random walk, *Oecologia* **56**, 234 (1983).
 - [16] P. Turchin, Translating foraging movements in heterogeneous environments into the spatial distribution of foragers, *Ecology* **72**, 1253 (1991).
 - [17] F. Bartumeus, M. G. E. da Luz, G. M. Viswanathan, and J. Catalan, Animal search strategies: a quantitative random-walk analysis, *Ecology* **86**, 3078 (2005).
 - [18] E. A. Codling, M. J. Plank, and S. Benhamou, Random walk models in biology, *J. R. Soc., Interface* **5**, 813 (2008).
 - [19] J. Gillis, Correlated random walk, *Math. Proc. Camb. Philos. Soc.* **51**, 639 (1955).
 - [20] E. Renshaw and R. Henderson, The correlated random walk, *J. Appl. Probab.* **18**, 403 (1981).
 - [21] L. Peliti and L. Pietronero, Random walks with memory, *Riv. Nuovo Cime.* **10**, 1 (1987).
 - [22] P. L. Krapivsky, S. Redner, and E. Ben-Naim, *A Kinetic View of Statistical Physics* (Cambridge University Press, New York, 2010).
 - [23] O. Peleg and L. Mahadevan, Optimal switching between geocentric and egocentric strategies in navigation, *R. Soc. Open Sci.* **3**, 160128 (2016).
 - [24] M. F. Shlesinger, Random searching, *J. Phys. A: Math. Theor.* **42**, 434001 (2009).

- [25] A. Reynolds, Cooperative random Lévy flight searches and the flight patterns of honeybees, *Phys. Lett. A* **354**, 384 (2006).
- [26] M. E. Wosniack, M. C. Santos, E. P. Raposo, G. M. Viswanathan, and M. G. Da Luz, The evolutionary origins of Lévy walk foraging, *PLoS Comput. Biol.* **13**, e1005774 (2017).
- [27] E. Raposo, S. Buldyrev, M. Da Luz, G. Viswanathan, and H. Stanley, Lévy flights and random searches, *J. Phys. A: Math. Theor.* **42**, 434003 (2009).
- [28] A. Reynolds, Optimal random Lévy-loop searching: New insights into the searching behaviours of central-place foragers, *Europhys. Lett.* **82**, 20001 (2008).
- [29] G. Berkolaiko and S. Havlin, Territory covered by n Lévy flights on d -dimensional lattices, *Phys. Rev. E* **55**, 1395 (1997).
- [30] G. M. Viswanathan, E. P. Raposo, F. Bartumeus, J. Catalan, and M. G. E. da Luz, Necessary criterion for distinguishing true superdiffusion from correlated random walk processes, *Phys. Rev. E* **72**, 011111 (2005).
- [31] F. Bartumeus, J. Catalan, U. L. Fulco, M. L. Lyra, and G. M. Viswanathan, Optimizing the encounter rate in biological interactions: Lévy versus Brownian strategies, *Phys. Rev. Lett.* **88**, 097901 (2002).
- [32] F. Bartumeus, Lévy processes in animal movement: An evolutionary hypothesis, *Fractals* **15**, 151 (2007).
- [33] G. Viswanathan, F. Bartumeus, S. V. Buldyrev, J. Catalan, U. Fulco, S. Havlin, M. Da Luz, M. L. Lyra, E. Raposo, and H. E. Stanley, Lévy flight random searches in biological phenomena, *Physica A* **314**, 208 (2002).
- [34] M. Santos, E. Raposo, G. Viswanathan, and M. da Luz, Can collective searches profit from Lévy walk strategies? *J. Phys. A: Math. Theor.* **42**, 434017 (2009).
- [35] R. Chadab and C. W. Rettenmeyer, Mass recruitment by army ants, *Science* **188**, 1124 (1975).
- [36] D. E. Jackson, M. Holcombe, and F. L. Ratnieks, Trail geometry gives polarity to ant foraging networks, *Nature (London)* **432**, 907 (2004).
- [37] M. Müller and R. Wehner, Path integration provides a scaffold for landmark learning in desert ants, *Curr. Biol.* **20**, 1368 (2010).
- [38] F. J. Acosta, F. López, and J. M. Serrano, Branching angles of ant trunk trails as an optimization cue, *J. Theor. Biol.* **160**, 297 (1993).
- [39] L. Li, H. Peng, J. Kurths, Y. Yang, and H. J. Schellnhuber, Chaos–order transition in foraging behavior of ants, *Proc. Natl. Acad. Sci. USA* **111**, 8392 (2014).
- [40] S. Wendt, N. Kleinhoelting, and T. J. Czaczkes, Negative feedback: Ants choose unoccupied over occupied food sources and lay more pheromone to them, *J. R. Soc., Interface* **17**, 20190661 (2020).
- [41] T. J. Czaczkes, A. Vollet-Neto, and F. L. Ratnieks, Prey escorting behavior and possible convergent evolution of foraging recruitment mechanisms in an invasive ant, *Behav. Ecol.* **24**, 1177 (2013).
- [42] D. M. Gordon and N. E. Heller, The invasive argentine ant *Linepithema humile* (Hymenoptera: Formicidae) in northern California reserves: From foraging behavior to local spread, *Myrmecol. News* **19**, 103 (2014).
- [43] J. D. Davidson and D. M. Gordon, Spatial organization and interactions of harvester ants during foraging activity, *J. R. Soc., Interface* **14**, 20170413 (2017).
- [44] C. R. Carroll and D. H. Janzen, Ecology of foraging by ants, *Annu. Rev. Ecol. Syst.* **4**, 231 (1973).
- [45] J. F. Traniello, Foraging strategies of ants, *Annu. Rev. Entomol.* **34**, 191 (1989).
- [46] R. Beckers, S. Goss, J.-L. Deneubourg, and J.-M. Pasteels, Colony size, communication and ant foraging strategy, *Psyche* **96**, 239 (1989).
- [47] Z. Reznikova, Ants personality and its dependence on foraging styles: Research perspectives, *Front. Ecol. Evol.* **9**, 661066 (2021).
- [48] E. O. Wilson, Communication by tandem running in the ant genus *Cardiocondyla*, *Psyche* **66**, 29 (1959).
- [49] M. Mglich, U. Maschwitz, and B. Hlldobler, Tandem calling: A new kind of signal in ant communication, *Science* **186**, 1046 (1974).
- [50] N. R. Franks and T. Richardson, Teaching in tandem-running ants, *Nature (London)* **439**, 153 (2006).
- [51] T. Sasaki, L. Danczak, B. Thompson, T. Morshed, and S. C. Pratt, Route learning during tandem running in the rock ant *Temnothorax albipennis*, *J. Exp. Biol.* **223**, jeb221408 (2020).
- [52] J.-C. Verhaeghe, Food recruitment in *Tetramorium impurum* (Hymenoptera: Formicidae), *Insectes Soc.* **29**, 67 (1982).
- [53] A. Dussutour, S. C. Nicolis, G. Shephard, M. Beekman, and D. J. Sumpter, The role of multiple pheromones in food recruitment by ants, *J. Exp. Biol.* **212**, 2337 (2009).
- [54] T. J. Czaczkes, C. Grüter, L. Ellis, E. Wood, and F. L. Ratnieks, Ant foraging on complex trails: route learning and the role of trail pheromones in *Lasius niger*, *J. Exp. Biol.* **216**, 188 (2013).
- [55] P. Amorim, Modeling ant foraging: A chemotaxis approach with pheromones and trail formation, *J. Theor. Biol.* **385**, 160 (2015).
- [56] D. J. Sumpter and M. Beekman, From nonlinearity to optimality: Pheromone trail foraging by ants, *Anim. Behav.* **66**, 273 (2003).
- [57] E. O. Wilson, Caste and division of labor in leaf-cutter ants (Hymenoptera: Formicidae: Atta) III. Ergonomic resiliency in foraging by *A. cephalotes*, *Behav. Ecol. Sociobiol.* **14**, 47 (1983).
- [58] E. O. Wilson, The relation between caste ratios and division of labor in the ant genus *Pheidole* (Hymenoptera: Formicidae), *Behav. Ecol. Sociobiol.* **16**, 89 (1984).
- [59] F. Bartumeus, J. Catalan, G. Viswanathan, E. Raposo, and M. da Luz, The influence of turning angles on the success of non-oriented animal searches, *J. Theor. Biol.* **252**, 43 (2008).
- [60] F. Bartumeus, D. Campos, W. S. Ryu, R. Lloret-Cabot, V. Méndez, and J. Catalan, Foraging success under uncertainty: Search tradeoffs and optimal space use, *Ecol. Lett.* **19**, 1299 (2016).
- [61] R. Palavalli-Nettimi and A. Narendra, Miniaturisation decreases visual navigational competence in ants, *J. Exp. Biol.* **221**, jeb177238 (2018).
- [62] B. D. Hughes, *Random Walks and Random Environments: Random Walks* (Oxford University Press, New York, 1995), Vol. 1.
- [63] G. H. Weiss, *Aspects and Applications of the Random Walk* (North Holland, New York, 1994).
- [64] A. Dvoretzky and P. Erdős, Some problems on random walk in space, in *Proceedings of the Second Berkeley Symposium on*

- Mathematical Statistics and Probability* (University of California Press, Berkeley, 1951), Vol. 2, pp. 353–368.
- [65] H. Larralde, P. Trunfio, S. Havlin, H. E. Stanley, and G. H. Weiss, Territory covered by n diffusing particles, *Nature (London)* **355**, 423 (1992).
- [66] H. Larralde, P. Trunfio, S. Havlin, H. E. Stanley, and G. H. Weiss, Number of distinct sites visited by n random walkers, *Phys. Rev. A* **45**, 7128 (1992).
- [67] M. F. Shlesinger, New paths for random walkers, *Nature (London)* **355**, 396 (1992).
- [68] H. Larralde, First-passage probabilities and mean number of sites visited by a persistent random walker in one- and two-dimensional lattices, *Phys. Rev. E* **102**, 062129 (2020).
- [69] J. Jun, J. W. Pepper, V. M. Savage, J. F. Gillooly, and J. H. Brown, Allometric scaling of ant foraging trail networks, *Evol. Ecol. Res.* **5**, 297 (2003).
- [70] C. Detrain and J.-L. Deneubourg, Collective decision-making and foraging patterns in ants and honeybees, *Adv. Insect Physiol.* **35**, 123 (2008).
- [71] M. Beekman, D. J. Sumpter, and F. L. Ratnieks, Phase transition between disordered and ordered foraging in Pharaoh's ants, *Proc. Natl. Acad. Sci. USA* **98**, 9703 (2001).
- [72] J. Buhl, D. J. Sumpter, I. D. Couzin, J. J. Hale, E. Despland, E. R. Miller, and S. J. Simpson, From disorder to order in marching locusts, *Science* **312**, 1402 (2006).
- [73] R. Sarfati, J. C. Hayes, and O. Peleg, Self-organization in natural swarms of *Photinus carolinus* synchronous fireflies, *Sci. Adv.* **7**, eabg9259 (2021).
- [74] J.-X. Shen, Z.-M. Xu, and E. Hankes, Direct homing behaviour in the ant *Tetramorium caespitum* (Formicidae, Myrmicinae), *Anim. Behav.* **55**, 1443 (1998).
- [75] R. A. Johnson, Learning, memory, and foraging efficiency in two species of desert seed-harvester ants, *Ecology* **72**, 1408 (1991).
- [76] N. Burgess, The 2014 Nobel Prize in Physiology or Medicine: A spatial model for cognitive neuroscience, *Neuron* **84**, 1120 (2014).
- [77] J. Sethna, *Statistical Mechanics: Entropy, Order Parameters, and Complexity*, Oxford Master Series in Physics Book Vol. 14 (Oxford University Press, New York, 2021).
- [78] T. Vicsek and A. Zafeiris, Collective motion, *Phys. Rep.* **517**, 71 (2012).
- [79] T. H. Gray and E. H. Yong, Effective diffusion in one-dimensional rough potential-energy landscapes, *Phys. Rev. E* **102**, 022138 (2020).
- [80] T. H. Gray and E. H. Yong, An effective one-dimensional approach to calculating mean first passage time in multi-dimensional potentials, *J. Chem. Phys.* **154**, 084103 (2021).
- [81] O. N. Bjørnstad, K. Shea, M. Krzywinski, and N. Altman, Modeling infectious epidemics, *Nat. Methods* **17**, 455 (2020).
- [82] M. Lu, M. K. Jolly, H. Levine, J. N. Onuchic, and E. Ben-Jacob, MicroRNA-based regulation of epithelial–hybrid–mesenchymal fate determination, *Proc. Natl. Acad. Sci. USA* **110**, 18144 (2013).
- [83] S. H. Strogatz, *Nonlinear Dynamics and Chaos: With Applications to Physics, Biology, Chemistry, and Engineering* (CRC Press, Boca Raton, FL, 2018).
- [84] S. D. Ryan, A model for collective dynamics in ant raids, *J. Math. Biol.* **72**, 1579 (2016).
- [85] W. Schiesser, *Time Delay ODE/PDE Models: Applications in Biomedical Science and Engineering* (CRC Press, Boca Raton, FL, 2019).